PHYSICAL REVIEW B **92**, 184408 (2015)

Anomalous structural behavior in the metamagnetic transition of FeRh thin films from a local viewpoint

Yuki Wakisaka,[1,2] Yohei Uemura,[2] Toshihiko Yokoyama,[2,1] Hiroyuki Asakura,[3] Hiroyuki Morimoto,[3]
Masao Tabuchi,[3] Daiki Ohshima,[4] Takeshi Kato,[5] and Satoshi Iwata[4]
[1]*Graduate School of Science, Nagoya University, Furo-cho, Chikusa-ku, Nagoya 464-8602, Japan*
[2]*Department of Materials Molecular Structure, Institute for Molecular Science, Myodaiji-cho, Okazaki 444-8585, Japan*
[3]*Synchrotron Radiation Research Center, Nagoya University, Furo-cho, Chikusa-ku, Nagoya 464-8603, Japan*
[4]*EcoTopia Science Institute, Nagoya University, Furo-cho, Chikusa-ku, Nagoya 464-8603, Japan*
[5]*Graduate School of Engineering, Nagoya University, Furo-cho, Chikusa-ku, Nagoya 464-8603, Japan*

(Received 19 June 2015; revised manuscript received 21 August 2015; published 9 November 2015)

The metamagnetic transition in FeRh thin films has been investigated via temperature-dependent x-ray-absorption fine-structure spectroscopy in order to gain correlations between magnetization and local electronic and geometric structures. According to the Fe and Rh K-edge x-ray-absorption near-edge structure (XANES), strong hybridization between Fe and Rh was revealed to exist. This Fe-Rh hybridization was observed to decrease during the phase transition from the antiferromagnetic (AFM) to ferromagnetic (FM) phases from the systematic change in the Fe K-edge XANES. In addition, only the Debye-Waller factor of the Fe-Fe pair in the AFM phase was observed to be considerably enhanced when compared with that in the FM phase, which was ascribed to local structural fluctuation inherent in the AFM phase. By considering the different features of the exchange interactions in Fe-Rh and Fe-Fe, this anomalous behavior is interpreted as being consistent with the recent theoretical study proposing the local fluctuations of spin and structure. Therefore, we consider that the local spin and Fe-Fe distance fluctuations play an important role in driving the metamagnetic transition, whereas the Fe-Rh hybridization correlates with the static stability of each magnetic phase.

DOI: 10.1103/PhysRevB.92.184408 PACS number(s): 75.50.Bb, 61.05.cj, 78.70.Dm

I. INTRODUCTION

The CsCl-type ordered FeRh alloy near equiatomic stoichiometry exhibits a metamagnetic transition, namely the antiferromagnetic (AFM) -ferromagnetic (FM) first-order phase transition, accompanied by an isostructural expansion at around 350 K [1,2]. Ever since its discovery in the late 1930s [1], much experimental and theoretical research has been done on this material. In recent years, it has gained considerable attention from the perspective of time-resolved experiments with ultrashort laser-pulse heating [3,4] and because of its potential applications to magnetic memory devices [5,6]. In the AFM phase, the Fe sublattice possesses a type-II AFM structure with a moment of $\sim 3\mu_B$ and no magnetic moment on Rh, while in the FM phase, the Fe and Rh sublattices possess moments of $\sim 3\mu_B$ and $\sim 1\mu_B$, respectively [7]. The transition temperature is readily influenced by various perturbations, including the Fe/Rh ratio [2], chemical doping [8], and external pressure or magnetic field [9,10].

Although a number of studies have investigated the metamagnetic transition in FeRh alloys, its physical origin and the essential interactions involved are still under debate. The magnetic contribution is regarded as essential for reducing the free energy of the FM phase compared with the AFM phase via a large entropy change [11,12] previously identified in initial studies [8,10,13]. However, evaluation of the electron contribution is elusive. Apart from several x-ray magnetic circular dichroism (XMCD) measurements [14,15], only a limited number of spectroscopic studies that directly probe the electronic states across the phase transition have been reported so far. One study used *in situ* soft-x-ray photoemission spectroscopy, wherein the core-level and valence-band spectra of the FeRh ultrathin film show little difference between the AFM and FM phases [16]. However, a recent study using bulk-sensitive hard-x-ray photoemission spectroscopy substantiated the modification of the valence band, which agrees with the density functional theory (DFT) calculation [17]. Furthermore, Hall coefficient measurements were interpreted as evidence of a considerable decrease in the density of states at the Fermi level [18,19].

To attain deeper insights into this phase transition, many theoretical studies have been performed, including first-principles calculations and Monte Carlo simulations [11,20–25]. Although the above-mentioned calculations adopted different methods and proposed different conclusions, they share the common concept that the emergence of the Rh magnetic moment plays a crucial role in stabilizing the FM phase. Some of the calculations [23,25] predict an intriguing picture of the exchange interaction between each atomic pair when the system is mapped to the Heisenberg spin model. In these calculations, the Fe-Rh exchange interaction J_{FeRh} is FM and quite robust against volume changes. Conversely, the Fe-Fe exchange interaction J_{FeFe} is AFM in both phases, but its absolute value depends strongly on volume changes. Consequently, the total balance of these two conflicting exchange interactions determines the final magnetic order of the system. The above feature of the exchange interactions indicates the correlation between spin and structural fluctuations. These two fluctuations were simultaneously treated by Derlet [24] in the Monte Carlo simulation and were speculated to grow only locally, triggering the phase transition. Thus, it must be quite interesting and important to capture these fluctuations experimentally to corroborate these theoretical pictures of the metamagnetic transition.

In the present study, considering the limited number of spectroscopic investigations directly probing the electronic states, and being inspired by the above theoretically proposed exchange-interaction picture and local fluctuations, we investigated the metamagnetic transition of FeRh using x-ray-absorption fine-structure (XAFS) spectroscopy. Generally, XAFS spectroscopy is one of the most powerful and suitable bulk-sensitive methods for locally detecting not only the electronic and geometric structures around specific atoms but also the bond-dependent structural fluctuations [26,27]. To date, only Miyanaga *et al.* [28] have reported the temperature behavior of the local structure of bulk FeRh across the phase transition using XAFS, wherein they have pointed out some symptoms of anomalous behaviors. Toward that end, the objective of our research is to capture the variation in the electronic state and the anomalous temperature behavior of each bond in correlation with the magnetization through XAFS spectroscopy, which will help to further enlighten the origin underlying this phenomenon.

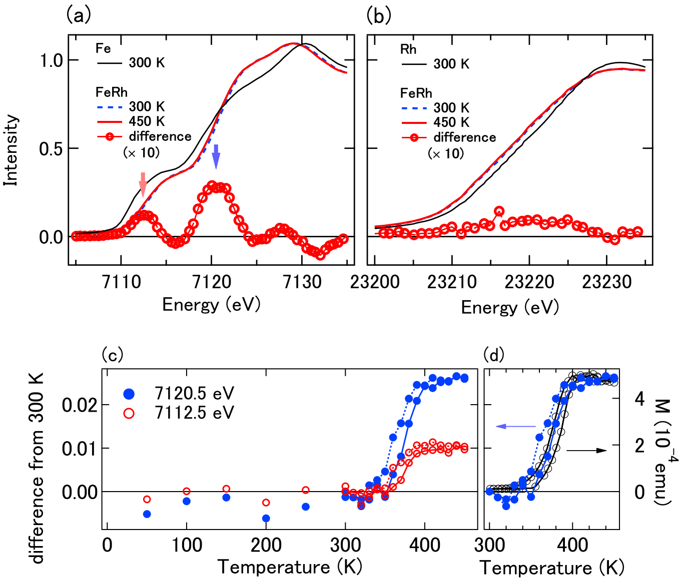

FIG. 1. (Color online) (a), (b) 300 K (AFM) and 450 K (FM) XANES of Fe (a) and Rh (b) *K* edges. The pure metal foil spectrum and difference spectrum are also shown. (c) The temperature dependence of the peak intensity of the difference spectra at 7112.5 eV (open red circle) and 7120.5 eV (filled blue circle). (d) Comparison of the XANES spectral intensity at 7112.5 eV (filled blue circle) with the magnetic moment *M* measured using SQUID at 300 Oe (open black circle). The solid and dotted lines for the XANES spectral intensities represent the heating and cooling processes during the measurement, respectively.

II. EXPERIMENTAL PROCEDURES

In a typical study, a 100-nm-thick $Fe_{49}Rh_{51}$ thin film was epitaxially grown on a single-crystal MgO(001) substrate by magnetron cosputtering of Fe and Rh targets. Here, a thin-film sample was selected for ease of performing future time-resolved XAFS experiments. During the deposition, the substrate was maintained at 300 °C at an argon pressure of 0.4 Pa followed by annealing for 30 min at 800 °C in order to facilitate the transformation to the CsCl-type structure [29]. Subsequently, after cooling to 100 °C, the thin film was coated with a 2-nm-thick tantalum passivation layer. The formation of a CsCl-type FeRh structure together with its high purity and crystallinity was confirmed using out-of-plane x-ray diffraction (XRD). The lattice constants were estimated to be $c = 3.001$ Å (out-of-plane) and $a = 2.983$ Å (in-plane), reflecting the $P4/mmm$ symmetry of the FeRh/MgO(001) thin film as previously reported [29]. The degree of substitutional disorder could be expressed by the order parameter S, which was evaluated to be 0.95 according to the peak intensities of the (001) and (002) Bragg reflections [30]. The occurrence of an AFM to FM phase transition at 385 K, consistent with the previously known transition temperature of FeRh/MgO(001) thin film [29], was verified by using a superconducting quantum interference device (SQUID, Quantum Design MPMS-7) dc magnetometer at 300 Oe and from the longitudinal magnetic optical Kerr effect.

The XAFS spectra for Fe and Rh *K* edges were obtained at beamlines 9A and NW10A using Si(111) and Si(311) monochromators, respectively, at the Photon Factory (or Photon Factory Advanced Ring) of the Institute of Material Structure Science, High Energy Accelerator Research Organization (KEK-PF). Pure Fe and Rh metal foils were measured as reference samples in the transmission mode, whereas FeRh thin film was measured in the fluorescence yield mode using a multielement Ge-SSD (solid-state detector). The sample was mounted with the x-ray electric field vector parallel to the $(1,1,\sqrt{2})$ direction (the basis of the FeRh lattice vectors was used). During the measurements, the sample was first heated from room temperature to 450 K and then cooled back to room temperature under a helium atmosphere. Subsequently, only for the Fe *K*-edge measurement, the sample was transferred into a helium compressor cryostat chamber, cooled to 50 K, and heated back to room temperature under vacuum. The XAFS calculations and analysis were performed using FEFF8.4 code [31] with the help of DEMETER and other software in the IFEFFIT package [32].

III. RESULTS AND DISCUSSION

A. X-ray-absorption near-edge structure

Figures 1(a) and 1(b) present the x-ray-absorption near-edge structures (XANES) of the Fe and Rh *K* edges of FeRh at 300 K (AFM) and 450 K (FM), respectively. The corresponding XANES spectra of pure Fe and Rh metal foils are also presented for reference. Comparing the XANES spectra of FeRh with those of pure Fe and Rh metal foils, the peak structures at approximately 7112.5 and 7120.5 eV are shifted to higher energies in the Fe *K* edge, whereas the entire edge is shifted to a lower energy in the Rh *K* edge. These results indicate electron transfer from Fe to Rh due to their strong hybridization and their difference in electronegativity (1.83 for Fe and 2.28 for Rh) [33]. In the case of iron oxides, this extent of the preedge shift in Fe *K*-edge XANES corresponds to ~0.5 formal valence [34,35]. This strong Fe-Rh hybridization supports the theoretical insight of its importance in the FM phase [23,25].

For the difference spectra of FeRh (the spectrum at 450 K subtracted by that at 300 K) in Figs. 1(a) and 1(b), a slight yet distinct increase is observed in the spectral weight at approximately 7112.5 and 7120.5 eV in the Fe *K*-edge XANES spectrum. Figure 1(c) depicts the temperature evolution of the Fe K-edge difference spectrum intensity at these two energies. Hysteresis loops with a transition temperature at 370 K are evidently observed for both the energies, suggesting the occurrence of AFM and FM phase separation from ∼360 to ∼400 K during the heating process and from ∼385 to ∼345 K during the cooling process. This behavior nearly corresponds to the magnetic temperature hysteresis loop obtained using SQUID under 300 Oe, as seen in Fig. 1(d), except for a downward shift by 15 K. The difference in transition temperature has also been found in the previous study of XMCD in photoemission electron microscopy (PEEM) [36]. This could have originated due to the fact that, under phase separation in PEEM (no field applied) and the current condition of SQUID (300 Oe), the magnetic moments of each local FM domain become unaligned and cancel each other. Consequently, the small FM island domains in the early (late) stage of heating (cooling) cannot be captured by the macroscopic magnetic measurements unless a sufficiently strong magnetic field is applied to align all the local FM domains. In contrast, the absolute value of the local XMCD-PEEM [36] and XAFS can be used to evaluate the area of the local FM domain irrespective of the alignment of each magnetic moment.

According to the local projected density of states calculated from FEFF8.4 (not shown), 7112.5 eV corresponds to the Fermi level at which the electronic states could be attributed to the Fe $4p$ states hybridized with Fe $3d$ and Rh $4d$ states, whereas the electronic states located ∼10 eV above the Fermi level (roughly corresponding to 7120.5 eV) are also hybridized with Fe $4s$ and Rh $5s$ states. The Fe K-edge XANES does not distinguish whether the spectral changes at 7112.5 and 7120.5 eV are caused by an increase in the Fe partial density of states at both energies or by a lower energy shift due to localization of electrons around Fe; both changes may be consistent with the experimental findings of the positive features in the difference spectra. However, both these changes could be caused by suppression of the Fe-Rh hybridization from the AFM to FM phases. Thus, the Fe electronic state was consequently revealed to vary depending on the hybridization with Rh in correlation with the metamagnetic transition. Unfortunately, any spectral difference associated with the Fe-Rh hybridization could not be observed in the Rh K-edge XANES due to the large broadening effect or the short lifetime of the Rh $1s$ core-hole final state and the limited energy resolution of the Si(311) monochromator.

This result agrees with the recent study on the bulk-sensitive hard-x-ray photoemission spectroscopy [17] in the sense that the Fe electronic state definitely varies between the AFM and FM phases. We also note here that no precursor feature appears concerning the Fe-Rh hybridization due to the absence of any anomalous behavior before or after the phase transition.

B. Extended x-ray-absorption fine structure

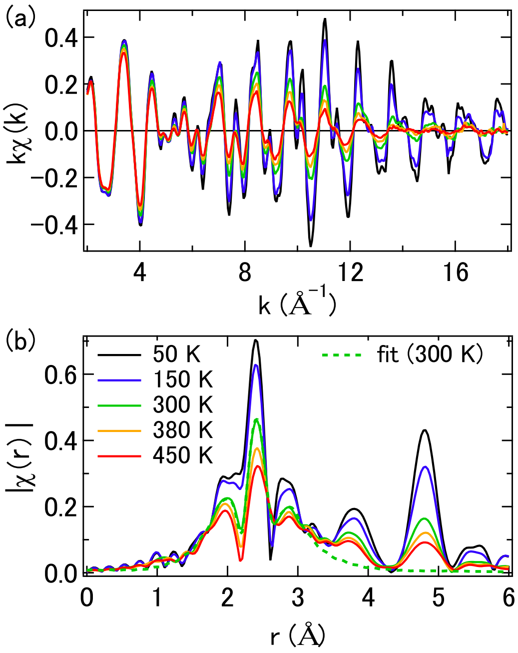

FIG. 2. (Color online) EXAFS spectra of the Fe K edge at different temperatures. (a) $k\chi(r)$, (b) $|\chi(r)|$. The fitted result for 300 K is also presented as a broken line.

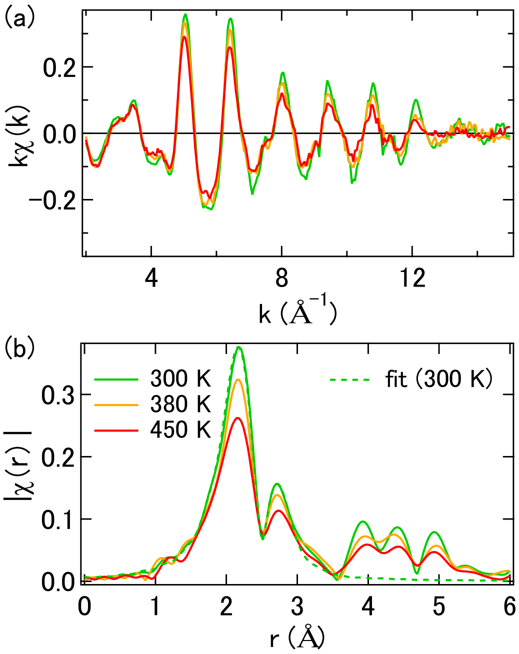

FIG. 3. (Color online) EXAFS spectra of the Rh K edge at different temperatures. (a) $k\chi(r)$, (b) $|\chi(r)|$. The fitted result for 300 K is also presented as a broken line.

Figures 2 and 3 present the extended x-ray-absorption fine-structure (EXAFS) oscillation functions $k\chi(k)$ and the corresponding Fourier transforms or the radial structural functions $|\chi(r)|$ of the Fe and Rh K edges. As is seen, clear oscillations can be observed over the entire temperature ranges. The ranges for the Fourier transform for the Fe and Rh K edges are $k = 2.6$–16.9 and 3.0–14.5 Å^{-1}, respectively. To extract the structural parameters, the radial structural functions in the range of 1.6–3.3 Å were fitted by the single-scattering EXAFS function, taking into consideration the two shells, which include the eight nearest Rh (Fe) atoms in the first

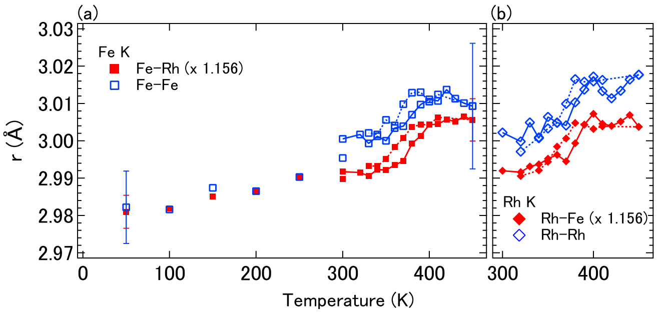

FIG. 4. (Color online) (a) The interatomic distances of Fe-Rh and Fe-Fe extracted from the Fe K-edge EXAFS. (b) The interatomic distances of Rh-Fe and Rh-Rh extracted from the Rh K-edge EXAFS. The solid and dotted lines represent the heating and cooling processes, respectively.

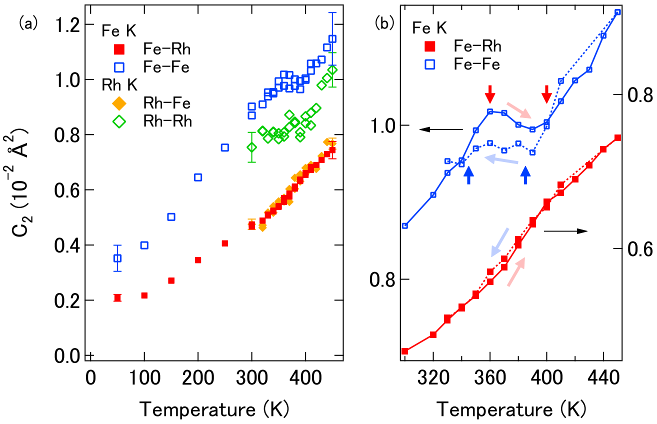

FIG. 5. (Color online) (a),(b) The Debye-Waller factors C_2 of Fe-Rh, Fe-Fe, and Rh-Rh extracted from the Fe and Rh K-edge EXAFS (a) and the enlarged view from 300 to 450 K for the Fe-Rh (Fe K edge) and Fe-Fe Debye-Waller factors (b) that exhibit clear hysteretic behaviors. The two darker red downward (blue upward) arrows in (b) indicate the beginning and end of the phase transition in the heating (cooling) process assigned from the Fe K-edge XANES intensity in Fig. 1(c). The solid and dotted lines represent the heating and cooling processes, respectively.

shell and the six next nearest Fe (Rh) atoms in the second shell for the Fe (Rh) K edge. The statistical distribution of the interatomic distances was expressed using the mean-square relative displacement or the Debye-Waller factor $C_2 = \langle (r - \langle r \rangle)^2 \rangle$ and the mean cubic relative displacement $C_3 = \langle (r - \langle r \rangle)^3 \rangle$. Although the actual crystal symmetry is $P4/mmm$, only one distance corresponding to Fe-Fe (Rh-Rh) was assumed in our fitting model of the crystal because the difference between the out-of-plane and in-plane distances is expected to be too small to separate by fitting (0.04 Å even at 450 K according to the following results). Therefore, the fitting result of the interatomic distance in the second shell is interpreted as the average of the out-of-plane and in-plane Fe-Fe (Rh-Rh) distances ($\frac{r_\parallel + r_\perp}{2}$) resulting from the present experimental orientation of the polarization $(1,1,\sqrt{2})$. This means that the experimentally observed Fe-Fe (Rh-Rh) distance could be scaled by the Fe-Rh distance by a factor of $1.156\,[= (\frac{a+c}{2})/r_{\text{Fe-Rh}}$, approximately equal to $2/\sqrt{3}]$ at 300 K. This factor is used in Fig. 4 assuming that the ratio between the out-of-plane and in-plane lattice constants remains the same as that at 300 K in the AFM phase. In fact, this assumption is violated in the FM phase for thin-film FeRh because only the out-of-plane direction is free from the substrate constraint. However, this effect is expected to be negligible in our present temperature range [37]. With respect to C_3, the Fe-Rh and Fe-Fe shells in the Fe EXAFS were fitted freely, while the Rh-Fe shell in the Rh EXAFS was fixed to the C_3 value of the Fe-Rh shell extracted from the Fe EXAFS at each temperature. The C_3 of the Rh-Rh shell was kept constant over the entire temperature range giving the random dispersion of the fitted values. Altogether, the Fe (Rh) EXAFS fitting had six (four) fitting parameters with the number of independent points $N_{\text{idp}} = 2\Delta k \Delta r/\pi + 2$ as 17 (14), where Δk and Δr are the ranges of the wave vector k and of the radial distance r used in the curve-fitting analysis based on the Fourier transformation. The R factors were below 1.2% for all the fittings, assuring their good fitness. The fitted results for 300 K are superposed in Figs. 2 and 3.

1. Interatomic distance

Figure 4 presents the extracted interatomic distances of Fe-Rh (Rh-Fe) and Fe-Fe (Rh-Rh). The Fe-Rh and Fe-Fe distances obtained from the Fe K-edge EXAFS undoubtedly exhibit a systematic behavior, correlated with the magnetic phase transition [Fig. 4(a)]. This behavior can be divided into three regions: a gradual expansion from 50 to 350 K, an evident hysteresis with a degree of 0.4% jump at approximately 370 K, and a much lower or negligible expansion above 400 K. The hysteretic behavior perfectly matches with that observed in the Fe K-edge XANES spectra shown in Fig. 1(c), and thus it corresponds to the magnetization. The 0.4% jump of the interatomic distances is the same as that of the 0.7% shift of the out-of-plane lattice constant in the thin-film XRD report [37], which corresponds to a 0.35% jump in the Fe-Rh distance and the average Fe-Fe distance in the present study. The extremely moderate expansion in the FM phase of FeRh is well known as the invar-like behavior [9,38] understood by the growing magnetic excitations, which compensate for the usual thermal expansion.

The previously reported XAFS result of bulk FeRh [28] has revealed some peculiar temperature behaviors with regard to the nearest-neighbor and next-nearest-neighbor distances, such as the deviation from their crystallographic interatomic-distance ratio. Here, a similar deviation is confirmed to show up even below the metamagnetic transition temperature, where the system is in a complete AFM phase. Figure 4(b) shows a less prominent but common tendency of the interatomic distances obtained from the Rh K-edge EXAFS, further assuring the structural transition.

2. Debye-Waller factor

Figure 5 presents the extracted Debye-Waller factors. The Debye-Waller factor of Fe-Rh exhibits normal behavior even during the phase transition. The Fe-Rh Debye-Waller factor is observed to increase rather monotonically with an increase in temperature due to the enhancement of the usual thermal vibrations. Although a slight hysteretic feature and an enhancement in the slope are observed due to the increase (decrease) of the Fe-Rh distance during the phase transition in Fig. 5(b), no noticeable anomalies can be detected before or after the phase transition.

In striking contrast to Fe-Rh, the Debye-Waller factors of Rh-Rh and Fe-Fe exhibit no increase or even a decrease during heating from the AFM to FM phases. The Fe-Fe Debye-Waller factor in Fig. 5(b) exhibits a clear peak at ~360 K in the heating process. The temperature of ~360 K does not correspond to the middle point of the AFM-to-FM transition, rather it corresponds to the beginning of the transition. Because the phase separation would give a maximum static fluctuation near the middle point of the phase transition [36,37,40], the present finding indicates that the maximum fluctuation is not caused by the AFM-FM phase separation but by the appearance of a fluctuation inherent in the AFM phase.

Such an anomalous behavior in the Fe-Fe Debye-Waller factor could be interpreted as a precursor effect pertinent to the phase transition, that is, the local fluctuations of spin and structure proposed in the recent theoretical paper [24], considering the different features of the exchange interactions in Fe-Rh and Fe-Fe. As mentioned in the Introduction, the AFM exchange interaction J_{FeFe} depends more strongly on volume change than the FM exchange interaction J_{FeRh} [23,25]. At a small volume, the AFM state is exclusively favored [23], and the local spin fluctuation in Fe-Fe should require the elongation of the Fe-Fe distance. If this local fluctuating elongation requires a longer Fe-Fe distance than the static FM Fe-Fe distance, a larger Debye-Waller factor of the Fe-Fe pair in the AFM state would be observed, as in Fig. 5(b). In contrast, the FM state more easily allows for the spin fluctuation because of the weakening of the Fe-Fe AFM exchange interaction [23], which is caused by the longer Fe-Fe distance in the FM state. In other words, the AFM Fe-Fe pair could be energetically present in the FM state without the relaxation of the Fe-Fe distance, resulting in a rather small Fe-Fe Debye-Waller factor in the FM phase. Therefore, the enhancement of the Fe-Fe Debye-Waller factor inherent in the AFM phase indicates that the local spin and Fe-Fe distance fluctuations act as a precursor, playing an important role for driving the metamagnetic transition. This finding clearly contrasts with the Fe-Rh hybridization showing no precursor feature in the preceding Fe K-edge XANES result, which is also supported by the observed normal behavior of the Fe-Rh Debye-Waller factor. Thus, Fe-Rh hybridization appears to correlate only with the static stability of each magnetic phase.

For the Rh atoms, they most likely do not completely follow the fast fluctuating Fe atoms, thereby leading to a much flatter temperature dependence of the Rh-Rh Debye-Waller factor. Note that the FM state is known to have stiffer lattice features than the AFM state by several measurements [9,12]; thus, the stiffness of the FM phase can be attributed to the characteristic of the Fe sublattice.

Although the behavior of the Debye-Waller factors was intuitively interpreted by referring to the recent theoretical calculation [23], precise discussion should be avoided because it does not address local spin fluctuations with varying interatomic distances. Thus, theoretical investigations including both local structural and magnetic fluctuations in both FM and AFM phases will be essential, as suggested by Derlet [24], for further understanding these Debye-Waller factors and the origin of the metamagnetic transition.

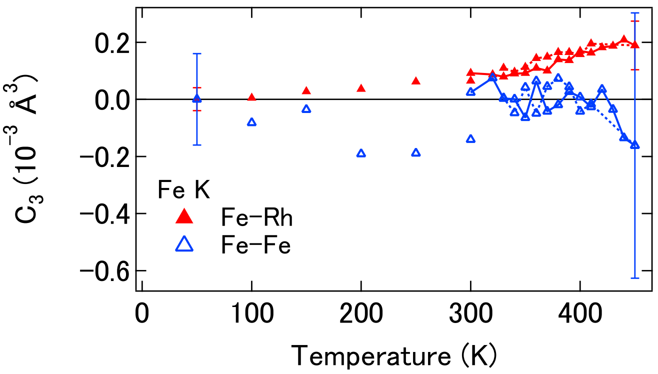

FIG. 6. (Color online) The mean cubic relative displacements C_3 of Fe-Rh and Fe-Fe extracted from the Fe K-edge EXAFS. The solid and dotted lines represent the heating and cooling processes, respectively.

Here, we should mention the static contribution of the Debye-Waller factors. According to temperature-dependent out-of-plane XRD results [40], it is reasonable to expect that the static distribution of the Fe-Fe distance is considerably larger at the middle of the phase transition than the AFM phase as mentioned above, although XRD only examines the entire average structure without atomic selectivity. Very recently, x-ray magnetic linear dichroism (XMLD) and PEEM (XMLD-PEEM) measurements using the Fe L edge were conducted to obtain information about the AFM domain structure [41]. This measurement provided local structural information specific to Fe and identified an interesting AFM domain structure even after the phase transition was completed. However, the correlation length of the domain structure was estimated to be 300 nm, which appears to be too large to contribute to the enhancement in our present Fe-Fe Debye-Waller factor in the AFM phase [42]. Although we could not exclude the possibility of static disorder in the AFM phase with very small or no correlation length, there is no available experimental data at present, showing static disorders that can explain the different temperature behaviors observed for the Fe-Rh and Fe-Fe Debye-Waller factors.

3. Mean cubic relative displacement

Let us finally discuss the behavior of C_3 of the Fe-Rh and Fe-Fe pairs extracted from the Fe K-edge EXAFS (Fig. 6). While the C_3 of Fe-Rh and its derivative are always positive as expected, the C_3 of Fe-Fe is peculiar. Although the error bar of C_3 is too large to discuss in detail, at least the following overall tendency could be observed. At low temperatures, it is negative and decreases with increasing temperature until it starts to increase at around 200–250 K up to 0 or a positive value. Following that, when the phase transition is completed, it decreases again. A similar trend in C_3 is also obtained in the previous XAFS study of bulk FeRh [39].

The intricate temperature dependence of Fe-Fe C_3 compared with Fe-Rh C_3 implies that the local Fe-Fe distance is not determined by normal thermal expansion in anharmonic crystals but is more strongly influenced by the effect of the local spins. In fact, its behavior could be qualitatively understood in accordance with the picture of the Fe-Fe exchange interaction J_{FeFe} and the local fluctuations of spin and structure, which we discussed in the previous subsection. The decrease in Fe-Fe C_3 at lower temperatures is consistent with the behavior of J_{FeFe}, whose distance dependence $\partial J_{\mathrm{FeFe}}/\partial r$ is considered to be positive [23,25], as long as all the local spin configurations are kept AFM. From 200 to 300 K, not only the usual thermal expansion but also the local FM and structural fluctuations start to show up, causing the Fe-Fe C_3 to increase. Intriguingly, this temperature region, which corresponds to 1–2 mRy, is close to the energy gap between the AFM and FM phases calculated using the local density approximation [11,20,21]. After the system becomes totally FM, it starts to decrease again due to the positive $\partial J_{\mathrm{FeFe}}/\partial r$ and the growing magnetic excitation or weakening of the FM order. However, a detailed calculation is inevitable to quantitatively interpret this behavior of C_3.

IV. SUMMARY

The present study investigates the metamagnetic transition in a CsCl-type ordered FeRh thin film using XAFS measurements. Concerning the electronic states, strong hybridization between Fe and Rh exists in FeRh, which decreases in the FM phase as compared with the AFM phase, without any evidence of a precursor. In addition, analysis of the observed Debye-Waller factors of Fe-Rh, Fe-Fe, and Rh-Rh revealed that only the Fe-Fe distance exhibited an enhanced fluctuation, which was attributed to the inherent nature of the AFM phase near the phase transition. This anomalous feature is interpreted as being consistent with the theoretically proposed local fluctuations of spin and structure by considering the different features of the exchange interactions in Fe-Rh and Fe-Fe. Therefore, the local spin and Fe-Fe distance fluctuations were revealed to play an important role for driving the metamagnetic transition, whereas the Fe-Rh hybridization correlates with the static stability of each magnetic phase. It will be extremely interesting to explore how these two different local features evolve dynamically through temporal heating and cooling; this will be left for future work.

ACKNOWLEDGMENTS

We would like to thank the members of the XAFS group of KEK-PF for their support in performing the XAFS measurements. We are also grateful to Dr. M. Fujiwara of the Institute for Molecular Science (IMS) for his kind support in SQUID measurements at the Instrument Center of IMS. We kindly appreciate T. Miyanaga for discussing the previous XAFS result of bulk FeRh. We would also like to thank Enago (www.enago.jp) for the English language review. A part of this study was supported by Nagoya University Nanofabrication Platform in Nanotechnology Platform Project sponsored by the Ministry of Education, Culture, Sports, Science and Technology (MEXT), Japan. The XAFS measurements at Photon Factory have been performed under the approval of the Photon Factory Program Advisory Committee (PF-PAC No. 2014G598 and 2014G046). We are grateful for the partial financial support of a Grant-in-Aid for Scientific Research (A) (No. 15H02173) from Japan Society for the Promotion of Science (JSPS).

---

[1] M. Fallot and R. Hocart, Rev. Sci. **77**, 498 (1939).
[2] G. Shirane, C. W. Chen, P. A. Flinn, and R. Nathans, Phys. Rev. **131**, 183 (1963).
[3] J.-U. Thiele, M. Buess, and C. H. Back, Appl. Phys. Lett. **85**, 2857 (2004).
[4] S. O. Mariager, F. Pressacco, G. Ingold, A. Caviezel, E. Möhr-Vorobeva, P. Beaud, S. L. Johnson, C. J. Milne, E. Mancini, S. Moyerman, E. E. Fullerton, R. Feidenhans'l, C. H. Back, and C. Quitmann, Phys. Rev. Lett. **108**, 087201 (2012).
[5] J.-U. Thiele, S. Maat, and E. E. Fullerton, Appl. Phys. Lett. **82**, 2859 (2003).
[6] R. O. Cherifi, V. Ivanovskaya, L. C. Philips, A. Zobelli, I. C. Infante, E. Jacquet, V. Garcia, S. Fusil, P. R. Briddon, N. Guiblin, A. Mougin, A. A. Ünal, F. Kronast, S. Valencia, B. Dkhil, A. Barthélémy, and M. Bibes, Nat. Mater. **13**, 345 (2014).
[7] G. Shirane, R. Nathans, and C. W. Chen, Phys. Rev. **134**, A1547 (1964).
[8] J. S. Kouvel, J. Appl. Phys. **37**, 1257 (1966).
[9] A. I. Zakharov, A. M. Kadomtseva, R. Z. Levitin, and E. G. Ponyatovskiĭ, Sov. Phys. JETP **19**, 1348 (1964).
[10] J. B. McKinnon, D. Melville, and E. W. Lee, J. Phys. C **3**, S46 (1970).
[11] R. Y. Gu and V. P. Antropov, Phys. Rev. B **72**, 012403 (2005).
[12] D. W. Cooke, F. Hellman, C. Baldasseroni, C. Bordel, S. Moyerman, and E. E. Fullerton, Phys. Rev. Lett. **109**, 255901 (2012).
[13] P. Tu, A. J. Heeger, J. S. Kouvel, and J. B. Comly, J. Appl. Phys. **40**, 1368 (1969).
[14] J. Chaboy, F. Bartolomé, M. R. Ibarra, C. I. Marquina, P. A. Algarabel, A. Rogalev, and C. Neumman, Phys. Rev. B **59**, 3306 (1999).
[15] C. Stamm, J.-U. Thiele, T. Kachel, I. Radu, P. Ramm, M. Kosuth, J. Minár, H. Ebert, H. A. Dürr, W. Eberhardt, and C. H. Back, Phys. Rev. B **77**, 184401 (2008).
[16] J.-S. Lee, E. Vescovo, L. Plucinski, C. M. Schneider, and C.-C. Kao, Phys. Rev. B **82**, 224410 (2010).
[17] A. X. Gray, D. W. Cooke, P. Krüger, C. Bordel, A. M. Kaiser, S. Moyerman, E. E. Fullerton, S. Ueda, Y. Yamashita, A. Gloskovskii, C. M. Schneider, W. Drube, K. Kobayashi, F. Hellman, and C. S. Fadley, Phys. Rev. Lett. **108**, 257208 (2012).
[18] Y. Kobayashi, K. Muta, and K. Asai, J. Phys.: Condens. Matter **13**, 3335 (2001).
[19] M. A. de Vries, M. Loving, A. P. Mihai, L. H. Lewis, D. Heiman, and C. H. Marrows, New J. Phys. **15**, 013008 (2013).
[20] V. L. Moruzzi and P. M. Marcus, Phys. Rev. B **46**, 2864 (1992).
[21] M. E. Gruner, E. Hoffmann, and P. Entel, Phys. Rev. B **67**, 064415 (2003).
[22] G. Ju, J. Hohlfeld, B. Bergman, R. J. M. van de Veerdonk, O. N. Mryasov, J.-Y. Kim, X. Wu, D. Weller, and B. Koopmans, Phys. Rev. Lett. **93**, 197403 (2004).
[23] L. M. Sandratskii and P. Mavropoulos, Phys. Rev. B **83**, 174408 (2011).

[24] P. M. Derlet, Phys. Rev. B **85**, 174431 (2012).
[25] J. Kudrnovský, V. Drchal, and I. Turek, Phys. Rev. B **91**, 014435 (2015).
[26] P. Pfalzer, G. Obermeier, M. Klemm, S. Horn, and M. L. denBoer, Phys. Rev. B **73**, 144106 (2006).
[27] R. Bindu, K. Maiti, S. Khalid, and E. V. Sampathkumaran, Phys. Rev. B **79**, 094103 (2009).
[28] T. Miyanaga, T. Itoga, T. Okazaki, and K. Nitta, J. Phys.: Conf. Ser. **190**, 012097 (2009).
[29] S. Maat, J.-U. Thiele, and E. E. Fullerton, Phys. Rev. B **72**, 214432 (2005).
[30] B. E. Warren, *X-Ray Diffraction* (Addison-Wesley, Reading, MA, 1969).
[31] B. Ravel and M. Newville, J. Synch. Radiat. **12**, 537 (2005).
[32] M. Newville, J. Synch. Radiat. **8**, 322 (2001).
[33] J. E. Huheey, *Inorganic Chemistry* (Harper & Row, New York, 1983).
[34] M. Kobayashi, H. Niwa, M. Saito, Y. Harada, M. Oshima, H. Ofuchi, K. Terakura, T. Ikeda, Y. Koshigoe, J. Ozaki, and S. Miyata, Electrochim. Acta **74**, 254 (2012).
[35] A. W. Brownrigg, G. Mountjoy, A. V. Chadwick, M. Alfredsson, W. Bras, J. Billaud, A. R. Armstrong, P. G. Bruce, R. Dominko, and E. M. Kelder, J. Mater. Chem. A **3**, 7314 (2015).
[36] C. Baldasseroni, C. Bordel, A. X. Gray, A. M. Kaiser, F. Kronast, J. Herrero-Albillos, C. M. Schneider, C. S. Fadley, and F. Hellman, Appl. Phys. Lett. **100**, 262401 (2012).
[37] S. O. Mariager, L. Le Guyader, M. Buzzi, G. Ingold, and C. Quitmann, arXiv:1301.4164.
[38] M. R. Ibarra and P. A. Algarabel, Phys. Rev. B **50**, 4196 (1994).
[39] T. Miyanaga (private communication).
[40] M. A. de Vries, M. Loving, M. McLaren, R. M. D. Brydson, X. Liu, S. Langridge, L. H. Lewis, and C. H. Marrows, Appl. Phys. Lett. **104**, 232407 (2014).
[41] C. Baldasseroni, C. Bordel, C. Antonakos, A. Scholl, K. H. Stone, J. B. Kortright, and F. Hellman, J. Phys.: Condens. Matter **27**, 256001 (2015).
[42] C.-M. Lin, T.-L. Hung, Y.-H. Huang, K.-T. Wu, M.-T. Tang, C.-H. Lee, C. T. Chen, and Y. Y. Chen, Phys. Rev. B **75**, 125426 (2007).